

THE DETERMINATION OF FREE VIBRATIONS OF LONGITUDINALLY-STIFFENED,
THIN-WALLED, CIRCULAR CYLINDRICAL SHELLS¹

W. Schnell and F. Heinrichsbauer

ABSTRACT

14284

Free vibrations of longitudinally-stiffened, circular cylindrical shells are investigated according to the linear theory. The basic equations of vibrations of orthotropic circular cylinders are derived and methods of solution (continuous, "blurred orthotropy": discontinuous, matrix method) are discussed. The method of conversion matrices takes into account the effect of discrete stiffening upon vibrational behavior. It permits development of equations of frequency in closed form and the simple determination of eigenforms. The results of theoretical investigations are compared with experimental values.


Author

Contents

1. Introduction
 2. Basic equations of vibrations of the orthotropic circular cylinder
 3. Solution of the basic equations
 - 3.1 Methods of solution
 - 3.2 Solution for blurred orthotropy
 4. Solution with conversion matrices
 - 4.1 Differential equations, formulas, boundary conditions
 - 4.2 Construction of the field matrix
 - 4.3 Stiffness conversion
 - 4.4 Transformation
 - 4.5 Equations of frequency and eigenforms
 5. Experimental determination of natural frequencies and free vibrational forms
 6. Results and discussion
- Bibliography

¹From the Institute of Strength of Materials of the German Aerospace Research Institute (DVL) Mülheim-Ruhr.

The present work was carried out with assistance of the German Research Organization.



1. Introduction

/2

The vibration of thin-walled structural units is important in various problems of aerospace statics. Thus, the fatigue behavior of plates under sonic stress (jet propulsion) depends upon the natural frequencies of the structure. Rocket shells can be excited to free vibrations (breathing modes) that for their part in conjunction with the other oscillatable parts of the flight structure react upon the control.

As a suitable model for aircraft and flight structures, thin-walled, circular cylindrical shells were preliminarily considered; these shells being stiffened by stringers. While the vibrations of isotropic cylindrical shells under various boundary conditions have been thoroughly clarified (Refs. 1, 2, 3) until the present, closely stiffened cylinders have been approximated by orthotropic calculation (Refs. 4, 5, 6). No investigations have been made concerning the effect of discrete stiffening. In the present paper, the vibrational behavior of discretely stiffened shells is theoretically and experimentally determined.

2. Basic Equation of Vibrations of Orthotropic Circular Cylinders

The investigations are based upon the following assumptions. The material of the ideal round cylinder is perfectly elastic, and wall thickness is small in proportion to the radius. Displacements are small in comparison to wall thickness, and shearing force deformation and the effect of rotational inertia are disregarded.

In Figure 1 the investigated circular cylindrical shell is presented with coordinate system and designations, as well as the cross-sectional measurements of a stringer. Coordinates of length and periphery are designated x and y , while z is radially measured positively toward the interior. The corresponding elastic displacements are designated u , v and w . Calculations are carried out with dimensionless coordinates $\xi = \frac{x}{r}$ and $\varphi = \frac{y}{r}$. The cylinder has a radius r , wall thickness t and length l . The thin-walled cylinder skin is stiffened on the inside by hat-formed stringers that are uniformly distributed over the periphery.

With the known reductions of Donnell (Ref. 7) the equations of motion for the shell element are:

$$\frac{1}{r} N_{\xi}' + \frac{1}{r} N_{\xi\varphi}' - \rho t \frac{\partial^2 u}{\partial t^2} = 0 \quad (2.1)$$

$$\frac{1}{r} N_{\xi\varphi}' + \frac{1}{r} N_{\varphi}' - \rho t \frac{\partial^2 v}{\partial t^2} = 0$$

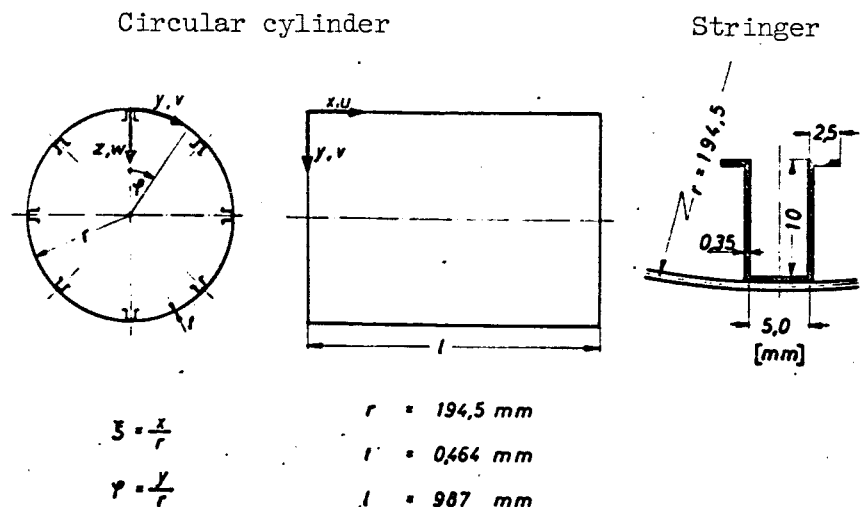


Figure 1. Designations and measurements of cylindrical shell and stringer

with $\frac{\partial}{\partial \xi}$, $\frac{\partial}{\partial \varphi}$, $\frac{\partial}{\partial t}$ derivative as a function of time.

In the last equation, shearing forces Q_ξ and Q_φ are eliminated by the application of moments. N_ξ , N_φ , M_ξ , etc. are variable sectional stresses occurring in the course of the vibration process. Instead of external

forces, inertial forces $qt \frac{\partial^2 u}{\partial t^2}$ etc., occur in the "conditions of equilibrium" (2.1); in this expression qt is the inertial mass per unit of middle surface of the stiffened cylinder.

With the assumption of an ideal elastic material, the linear law of elasticity for tractions of the middle surface of the orthotropic shell whose principal directions of rigidity coincide with the coordinate axes, is expressed as:

$$\begin{pmatrix} \epsilon_\xi \\ \epsilon_\varphi \\ \gamma_{\xi\varphi} \end{pmatrix} = \begin{pmatrix} C_{11} & C_{12} & 0 \\ C_{21} & C_{22} & 0 \\ 0 & 0 & C_{33} \end{pmatrix} \cdot \begin{pmatrix} N_\xi \\ N_\varphi \\ N_{\xi\varphi} \end{pmatrix} \quad (2.2)$$

and for sectional moments

$$\begin{pmatrix} M_{\xi} \\ M_{\varphi} \\ M_{\xi\varphi} \end{pmatrix} = \begin{pmatrix} D_{11} & D_{12} & 0 \\ D_{21} & D_{22} & 0 \\ 0 & 0 & 2D_{33} \end{pmatrix} \cdot \begin{pmatrix} \kappa_{\xi} \\ \kappa_{\varphi} \\ \kappa_{\xi\varphi} \end{pmatrix} \quad (2.3)$$

Thereby C_{ij} represents the reciprocal values of longitudinal stiffness or of modulus of elasticity for shear (Ref. 8) that in the case of isotropic material are converted into

$$\begin{aligned} C_{11} &= C_{22} = \frac{1}{Et} \\ C_{12} &= C_{21} = -\frac{\nu}{Et} \\ C_{33} &= \frac{1}{Gt} = \frac{2(1+\nu)}{Et} \end{aligned} \quad (2.4)$$

D_{ij} represents bending or torsional stiffness that in isotropic shells are:

$$\begin{aligned} D_{11} &= D_{22} = \frac{Et^3}{12(1-\nu^2)} \\ D_{12} &= D_{21} = \frac{\nu Et^3}{12(1-\nu^2)} \\ D_{33} &= \frac{Gt^3}{12} = \frac{1-\nu}{2} \frac{Et^3}{12(1-\nu^2)} \end{aligned} \quad (2.5)$$

In addition to conditions of equilibrium and the law of elasticity, the geometric interdependence of deformation strains and displacements, whereby only linear terms (linear theory) are considered:

$$\begin{aligned} \varepsilon_{\xi} &= \frac{1}{r} u' \\ \varepsilon_{\varphi} &= \frac{1}{r} (v' - w) \\ \gamma_{\xi\varphi} &= \frac{1}{r} (u' + v') \end{aligned} \quad (2.6)$$

Alternations of curvature of shells can be approximated according to Donnell (Ref. 7) with the values for thin flat plates:

$$\begin{aligned} \kappa_{\xi} &= \frac{1}{r^2} w'' \\ \kappa_{\varphi} &= \frac{1}{r^2} w'' \\ \kappa_{\xi\varphi} &= \frac{1}{r^2} w'' \end{aligned} \quad (2.7)$$

A system of linear partial differential equations for elastic displacements u , v , w in longitudinal, peripheral and radial directions is developed for vibrating orthotropic circular cylindrical shells from conditions of equilibrium (2.1), law of elasticity (2.2), (2.3) and geometry (2.6), (2.7):

$$\begin{aligned} [C_{22} u'' - C_{12} (v'' - w')] + \frac{C^2}{C_{33}} (u'' + v'') - C^2 g t r^2 \frac{\partial^2 u}{\partial t^2} &= 0 \\ [-C_{21} u' + C_{11} (v'' - w')] + \frac{C^2}{C_{33}} (u'' + v'') - C^2 g t r^2 \frac{\partial^2 v}{\partial t^2} &= 0 \quad (2.8) \\ \frac{C^2}{r^2} [D_{11} w'' + (D_{12} + D_{21} + 4D_{33}) w'' + D_{22} w''] - \\ - [-C_{21} u' + C_{11} (v'' - w')] + C^2 g t r^2 \frac{\partial^2 w}{\partial t^2} &= 0 \end{aligned}$$

with $C^2 = C_{11} C_{22} - C_{12} C_{21}$

3. Solution of the Basic Equations

3.1 Methods of Solution

The present system of linear partial differential equations (2.8) can be precisely solved for a purely orthotropic material (e.g., plywood) by selection of a suitable formula. In case of discrete stiffening by means of stringers solution can be attained by:

- 1) continuous calculation ("blurred orthotropy")
- 2) discontinuous calculation (matrix methods)

3.2 Solution for "Blurred Orthotropy"

In the first method the discretely stiffened cylinder is approximated by laying stringers on the skin. The degree of accuracy of such an approximation will naturally depend upon the number of stringers, i.e., the more stringers laid on, the closer will be the approximation.

For the deformation functions u , v , w in the basic equation (2.8), product expressions from circular functions with unknown amplitudes U , V , W are selected:

$$\begin{aligned}
 u &= U \cos n\varphi \cos \bar{m} \xi \sin \omega t \\
 v &= V \sin n\varphi \sin \bar{m} \xi \sin \omega t \\
 w &= W \cos n\varphi \sin \bar{m} \xi \sin \omega t
 \end{aligned}
 \tag{3.1}$$

Thereby $\bar{m} = m \frac{\pi r}{l}$ with m = the number of half periods and n = number

/6

of vibrations in the direction of the periphery. After substitution in (2.8) there is developed a linear homogeneous system of equations for the amplitudes; the vanishing coefficients determinant (frequency determinant) yields the natural frequencies as roots of a cubic equation:

$$\lambda^3 + \Lambda_2 \lambda^2 + \Lambda_1 \lambda + \Lambda_0 = 0 \tag{3.2}$$

with the eigenvalue $\lambda_1 = \frac{qr^2}{E} (1-v^2) w_1^2$ as a dimensionless natural angular frequency w_1 . The three interrelated natural frequencies (cf. Figure 2)

are three characteristic vibrational forms of equal number and arrangement of nodal lines, of which amplitude ratio $U:V:W$ yields a representation. In addition to distinct vibrations in the longitudinal and peripheral direction of the cylinder, there is a distinct transverse vibration in a radial direction at high frequencies. This transverse vibration is associated with the minimum natural frequency (minimum root of the cubic equation). This transverse vibration, because of its proximity to technical natural frequencies, is of particular importance. If it is to be determined advantageously, the factors of inertia in the longitudinal and

peripheral directions (terms with $\frac{\partial^2 u}{\partial t^2}$ and $\frac{\partial^2 v}{\partial t^2}$) can be disregarded in the conditions of equilibrium. The cubic eigenvalue equation then assumes a linear form:

$$\bar{\Lambda}_1 \lambda + \Lambda_0 = 0 \tag{3.3}$$

Another linearization is possible when we replace the cubic parabola by means of its tangent to point $\lambda = 0$; i.e., the quadratic and cubic term in (3.2) cancels:

$$\Lambda_1 \lambda + \Lambda_0 = 0 \tag{3.4}$$

The two linearizations are differentiated only in the term at λ ; the difference, however, is small enough to be disregarded.

Figure 2 illustrates the represented state for the example of a blur-calculated cylinder with 4 stringers. The three interrelated natural frequencies f_1 are plotted logarithmically in Hertzian units (as

roots of the cubic equation) as abscissas against the number of vibrations n in the peripheral direction. As a parameter the number of half periods m is entered in the longitudinal direction. For better orientation, the frequencies belonging to a specific m for integral values of n are interconnected by dashed lines. It will be observed that the frequencies of the longitudinal vibrations in the longitudinal and peripheral direction lie broadly above the technically interesting lower natural frequencies of the radial vibration. /7

4. Solution with Conversion Matrices

As already indicated, the degree of approximation by application of stringers on the skin increases with the number of applied stringers. In order to investigate the relationship in the case of few stringers and principally to clarify the effect of discrete stiffening upon the vibrational behavior of the circular cylindrical shell, the method of conversion matrices is available. In this case the structural parts of the stiffened cylinder, isotropic shell field + stringers, are first considered separately.

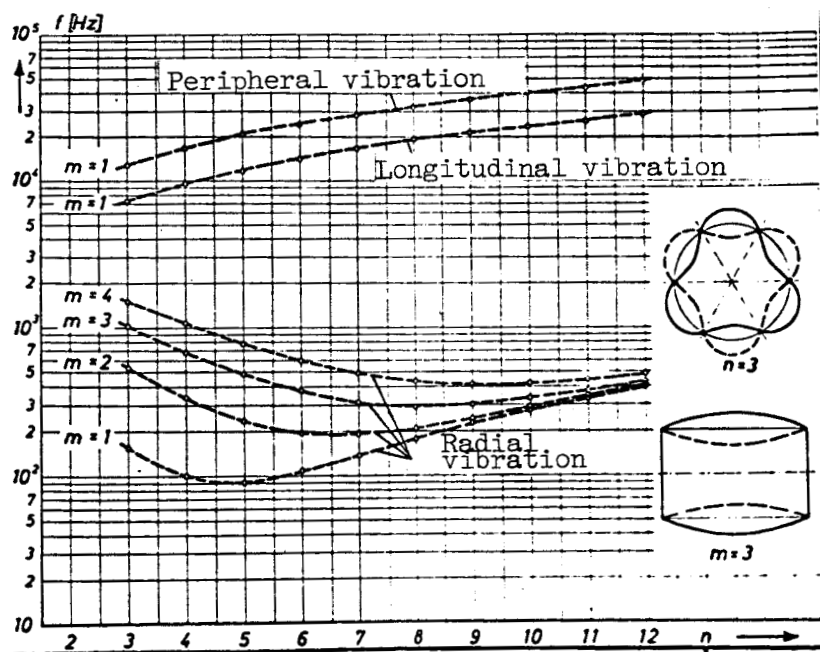


Figure 2. Natural frequencies of a stiffened cylinder
 $j = 4\sqrt{L}$ (blurred orthotropy)

4.1 System of Differential Equations, Formula for Solution, Boundary Conditions

The basic equations of vibration of orthotropic circular cylindrical shells (2.8) are rewritten for the isotropic case. With a temporal periodic formula for displacement functions u, v, w :

$$\begin{aligned} u &= u(\xi, \varphi) \sin \omega t \\ v &= v(\xi, \varphi) \sin \omega t \\ w &= w(\xi, \varphi) \sin \omega t \end{aligned} \quad (4.1)$$

there are developed 3 linear partial differential equations for u, v, w with λ as eigenvalue: /8

$$\lambda u + u'' + \frac{1-\nu}{2} u'' + \frac{1+\nu}{2} v'' - \nu w' = 0 \quad (4.2)$$

$$0 = \dots \quad (4.3)$$

$$0 = \dots \quad (4.4)$$

with
$$k = \frac{\xi^2}{12r^2}, \quad \Delta = \left(\frac{\partial^2}{\partial \xi^2} + \frac{\partial^2}{\partial \varphi^2} \right)$$

Equations (4.2) to (4.4) agree, with consideration of Donnell's reductions, with those of Flügge (Ref. 9).

On previously mentioned grounds, the inertial members in the longitudinal and peripheral direction (λ terms in (4.2) and (4.3)) can be disregarded. After elimination of v or u , equations (4.2) and (4.3) assume the forms:

$$\Delta \Delta u = -(w''' - \nu w''') \quad (4.5)$$

$$\Delta \Delta v = w''' + (2 + \nu) w'' \quad (4.6)$$

where the displacement components u and v alone are dependent upon radial displacement w . Equations (4.5) and (4.6) in (4.4) yield:

$$k \Delta \Delta \Delta \Delta w - \lambda \Delta \Delta w + (1 - \nu^2) w^{\text{IV}} = 0 \quad (4.7)$$

This linear partial differential equation of the 8th order has the radial displacement w as sole dependent variable.

The equations (4.5), (4.6) are used later for construction of a vector of state.

The isotropic shell field of the cylinder extends between the stringers. For its radial displacement w in the course of vibration, taking into account the stringers distributed over the periphery, we set down the formula:

$$w(\xi, \varphi) = W e^{\mu \varphi} \sin \bar{m} \xi \quad (4.8)$$

Formula (4.8) fulfills the boundary conditions with $\xi = 0$ and $\xi = \frac{1}{r}$

$$v = w = 0 \quad N_{\xi} = M_{\xi} = 0 \quad (4.9)$$

and therefore it fits a shell that is articulatedly borne at the boundaries on two plates that are rigid in their planes but in a direction perpendicular to this they are slack. These bearing relationships are taken into consideration in the investigation. /9

When formula (4.8) is written into equation (4.7) the result is an eigenvalue equation of the 8th order for the isotropic shell field:

$$k(\mu^2 - \bar{m}^2)^4 - \lambda(\mu^2 - \bar{m}^2)^2 + (1 - \nu^2)\bar{m}^4 = 0, \quad (4.10)$$

whose eight roots when opposed by pairs are equal;

$$\mu_{1,2} = \pm \sqrt{\bar{m}^2 + \sqrt{\frac{\lambda}{2k} (1 + \sqrt{1 - \alpha})}}, \quad \mu_{5,6} = \pm \sqrt{\bar{m}^2 - \sqrt{\frac{\lambda}{2k} (1 + \sqrt{1 - \alpha})}} \quad (4.11)$$

$$\mu_{3,4} = \pm \sqrt{\bar{m}^2 + \sqrt{\frac{\lambda}{2k} (1 - \sqrt{1 - \alpha})}}, \quad \mu_{7,8} = \pm \sqrt{\bar{m}^2 - \sqrt{\frac{\lambda}{2k} (1 - \sqrt{1 - \alpha})}}$$

with

$$\alpha = \frac{(1 - \nu^2) \bar{m}^4 4k}{\lambda^2}$$

It can be demonstrated that:

$$\sqrt{\sqrt{\frac{\lambda}{2k} (1 + \sqrt{1-\alpha})} - \bar{m}^2} = n$$

is valid for the closed isotropic circular cylindrical shell

(n = number of vibrations in the peripheral direction)

Thus the eigenvalue equation (4.10) is transformed into a simple linear form:

$$k(\bar{m}^2 + n^2)^4 - \lambda(\bar{m}^2 + n^2)^2 + (1 - \nu^2)\bar{m}^4 = 0 \quad (4.12)$$

From $\frac{\partial \lambda}{\partial n^2} = 0$

$$\lambda_{min} = 2\bar{m}^2 \sqrt{(1 - \nu^2)k} \quad (4.13)$$

results as minimum natural frequency for each selected number of half periods m in a longitudinal direction.

Since equation (4.13) is valid for unstiffened isotropic shells, we substitute the stiffened shell:

$$0 < \alpha \leq 1$$

Then $\mu_{1, 2}$ and $\mu_{3, 4}$ and the internal roots in $\mu_{5, 6}$ and $\mu_{7, 8}$ are definitely real. With roots (4.11) the solution formula (4.8) can be written as follows:

$$w(\xi, \varphi) = \sum_{i=1,3,5}^{i=7} (W_i \cos \mu_i \varphi + W_{i+1} \sin \mu_i \varphi) \sin \bar{m} \xi \quad (4.14)$$

4.2 Construction of the Field Matrix

The traditional classic approach to further solution is characterized by integration by sectors, determination by fields of the unknown amplitudes of vibration by boundary and transformation conditions, determination of natural frequencies from a homogeneous system of equations. Because of the complexity of the problem this approach is hardly practicable.

In contrast, the method of conversion matrices offers the possibility of a simpler, comprehensible solution of the problem of free vibrations of longitudinally stiffened circular cylindrical shells.

By means of solution formula (4.14) for radial displacement w and of differential equations (4.5), (4.6) for u and v , the vector of state is constructed whose elements consist of forces and displacements that are equal in dimension.

$$110_y = \begin{pmatrix} \tilde{u} \\ -10 \end{pmatrix}_y = \begin{pmatrix} N \\ U' \\ W \\ (-M) \\ (-T') \\ V \\ W' \\ Q \end{pmatrix}_y \quad (4.15)$$

Thereby $N = \frac{N_\varphi \cdot r}{Et\bar{m}^4}$ with N_φ = axial force/unit of length in the peripheral direction.

$$U' = \frac{u'}{\bar{m}^2} \quad \text{with } u = \text{longitudinal displacement} \quad /11$$

$$W = w \quad \text{with } w = \text{radial displacement}$$

$$M = \frac{M_\varphi 12(1-v^2)r^2}{Et^3} \quad \text{with } M_\varphi = \text{moment/unit of length in the peripheral direction}$$

$$T' = \frac{N'_{\varphi z} r}{Et\bar{m}^4} \quad \text{with } N_{\varphi z} = \text{shearing force/unit of length in the longitudinal direction}$$

$$V = v \quad \text{with } v = \text{peripheral displacement}$$

$$W' = w' \quad \text{with } w' = \text{inclination of displacement function } w \text{ in the peripheral}$$

$$Q = \frac{\bar{Q}_\varphi 12(1-v^2)r^3}{Et^3} \quad \text{with } \bar{Q}_\varphi = \text{substituted shearing force/unit of length in the peripheral direction}$$

The derivations in U' and T' have the effect that the same circular function $\sin \bar{m}\xi$ appears as a factor in all vector components and hence with further calculation it can be disregarded. The combination of each 4 vector components as u and w in matrix operations proves to be an advantageous form of notation.

The vector components of the vector of state in the field (at φ) are combined via the field matrix \mathcal{F} with the vector components at the beginning of the field (at $\varphi = 0$):¹

$$M\varphi = \begin{bmatrix} \tilde{u} \\ \tilde{w} \end{bmatrix}_{\varphi} = \begin{bmatrix} N \\ U' \\ W \\ (-M) \\ (-T') \\ V \\ W' \\ Q \end{bmatrix}_{\varphi} = \mathcal{F} \cdot \begin{bmatrix} N \\ U' \\ W \\ (-M) \\ (-T') \\ V \\ W' \\ Q \end{bmatrix}_0 = \mathcal{F} \cdot M\varphi_0 \quad (4.16)$$

Field matrix \mathcal{F} is an 8-line quadratic matrix the elements of which are combined as sums of hyperbolic functions. For example:

/12

$$f_{11} = \frac{1}{2(\psi - \phi)} \left\{ -\frac{B-A}{B} \phi \operatorname{sh} \mu_1 \varphi + \frac{C-A}{C} \psi \operatorname{sh} \mu_3 \varphi - \frac{A+B}{B} \phi \operatorname{sh} \mu_5 \varphi + \frac{A+C}{C} \psi \operatorname{sh} \mu_7 \varphi \right\}$$

and

$$f_{12} = \frac{1}{2(\psi - \phi)} \left\{ \frac{\phi \psi}{\mu_1 B} \operatorname{sh} \mu_1 \varphi - \frac{\phi \psi}{\mu_3 C} \operatorname{sh} \mu_3 \varphi - \frac{\phi \psi}{\mu_5 B} \operatorname{sh} \mu_5 \varphi + \frac{\phi \psi}{\mu_7 C} \operatorname{sh} \mu_7 \varphi \right\}$$

¹Because of lack of time a detailed presentation of all subsequent operations must be dispensed with in the present report: these details are reserved for a DVL report.

The transformation from field boundary into field can be summarized in matrix notation as follows:

$$\underbrace{\begin{bmatrix} \ddot{w} \\ 10 \end{bmatrix}}_{ND\varphi} = \underbrace{\begin{bmatrix} 1 & \begin{bmatrix} \delta & 0 \\ 0 & \gamma \end{bmatrix} & \begin{bmatrix} \varphi_0 & 0 \\ 0 & \varphi_0 \end{bmatrix} \\ 2(\psi-\phi) & 0 & \varphi \end{bmatrix}}_{\mathcal{F}} \underbrace{\begin{bmatrix} (\mathcal{L}\sigma/\mu\varphi)_D & (\frac{\mathcal{L}\mu\mu\varphi}{\mu})_D \\ (\mu\mathcal{L}\mu\mu\varphi)_D & (\mathcal{L}\sigma/\mu\varphi)_D \end{bmatrix}}_{\mathcal{F}} \underbrace{\begin{bmatrix} \mathcal{Z} & 0 \\ 0 & \mathcal{Z} \end{bmatrix}}_{ND0} \cdot \underbrace{\begin{bmatrix} \ddot{w} \\ 10 \end{bmatrix}}_{ND0} \quad (4.17)$$

whereby δ, γ column matrices
 φ, \mathcal{Z} line matrices
 $\varphi_0, (\mathcal{L}\sigma/\mu\varphi)_D$, etc. diagonal matrices

4.3 Stiffness Conversion

The stiffness conversion is summarized by a conversion matrix that takes into account the effect of transverse force bending and of the vibrating mass of the stringer. Only the transverse force changes before and after stiffening with respect to the transverse force difference whose magnitude depends upon radial displacement w (3rd component of u):

$$\underbrace{\begin{bmatrix} \ddot{w} \\ 10 \end{bmatrix}}_{ND\varphi_{j+1}} = \underbrace{\begin{bmatrix} \mathcal{L} & 0 \\ 0000 & \\ 0000 & \mathcal{L} \\ 0000 & \\ 00\bar{\kappa}0 & \end{bmatrix}}_{\mathcal{H}} \cdot \underbrace{\begin{bmatrix} \ddot{w} \\ 10 \end{bmatrix}}_{ND\varphi_j} \quad (4.18)$$

whereby

$$\bar{\kappa} = \kappa - \lambda \frac{F}{k r t}$$

$$\kappa = \frac{E_{sr}}{E_H} \frac{J_x}{t^3 r} \frac{1}{m^4} 12 (1 - \nu^2)$$

with F = area of section of the stringers
 J_x = moment of inertia of the stringers

/13

The first summand at \bar{n} expresses the effect of transverse force bending, and the second that of the vibrating mass of the stringer.

4.4 Transformations

In the equation (4.17) $\bar{n}D_y = \tilde{f} \cdot nD_0$ the matrix product is

$$\tilde{f}_1 nD = \left[\begin{array}{c|c} \tilde{f} & 0 \\ \hline 0 & \tilde{f} \end{array} \right] \left[\begin{array}{c} \bar{n} \\ \bar{n} \end{array} \right] \quad (4.19)$$

If the vector of state w is converted by means of transform matrix \tilde{f}_1 into vector of state \bar{w} , the transformed field matrix \tilde{f} will be significantly simplified:

$$\underbrace{\tilde{f}_1 nD_y}_{\bar{n}D_y} = \underbrace{\tilde{f}_1 \tilde{f} \tilde{f}_1^{-1}}_{\tilde{f}} \cdot \underbrace{\tilde{f}_1 nD_0}_{\bar{n}D_0} \quad (4.20)$$

By virtue of the structure of field matrix \tilde{f} a further transformation is available with transform matrix:

$$\tilde{f}_2 = \left[\begin{array}{c|c} \xi & 0 \\ \hline (\xi \otimes \mu \varphi)_D & \left(\frac{\xi \otimes \mu \varphi}{\mu} \right)_D \end{array} \right] \quad (4.21)$$

$$\underbrace{\tilde{f}_2 \bar{n}D_y}_{\bar{\bar{n}}D_y} = \underbrace{\tilde{f}_2 \tilde{f} \tilde{f}_2^{-1}}_{\bar{\bar{f}}} \cdot \underbrace{\tilde{f}_2 \bar{n}D_0}_{\bar{\bar{n}}D_0} \quad (4.22)$$

The twice transformed field matrix then yields the simple form

$$\bar{\bar{f}} = \begin{pmatrix} 0 & \mathcal{E} \\ -\mathcal{E} & \alpha \end{pmatrix} \quad (4.23)$$

with $A = (2L\sigma/\mu\varphi)_D$, diagonal matrix, and E as unit matrix. /14

In an analogous manner the stiffness matrix is twice transformed. $\bar{w}_j + 1 = \bar{\mathcal{H}} \cdot \bar{w}_j$. The conversion matrix $\bar{\mathcal{H}} \cdot \bar{f}$ in conversion from field beginning via field and stringer includes a form similar to $\bar{\bar{f}}$. Because of its simple construction the matrix operation can be followed in the conversion mechanism in this clear comprehensible form, and for the second time the linear equation system resulting at the end breaks up and can easily be solved in closed form.

4.5 Frequency Equations and Eigenforms

After one rotation about the entire cylinder, when the field and stiffness conversion again reaches its point of departure, the beginning and end vectors must be equipollent. From this condition there arises a homogeneous system of equations whose coefficient determinants must vanish. Numerical difficulties that occur in calculation of these determinants can be avoided if the conversion is not carried out over the entire shell. The requirement that after one complete rotation the beginning and end vectors must be identical can also be met by the possible solution that after one, two or four fields – depending upon the number of stringers in question – the vector of state is equal or opposite to the beginning vector.

Because of the simple form of the field and stiffness conversion it is possible in this way to derive frequency equations in a general form. Using the frequencies thus calculated, the vibration forms in the individual fields can be determined by reverse transformation. The numerical calculations for the example of a longitudinally stiffened vibrating circular cylindrical shell were performed on an IBM 1620 digital computer.

5. Experimental Determination of the Natural Frequencies and Free Vibration Forms

In order to obtain information concerning accuracy and value of the theory, we performed experiments that paralleled the calculations.

Figure 3 shows the experimental apparatus. The experimental cylinder of dynamo sheet could be completely turned about its longitudinal axis, with connection - for simulation of the selected bearing conditions (articulated bearing) - at the edges by a diaphragm. It was continuously excited by variable frequencies by an electromagnet mounted to slide on a U-shaped support. The vibrations in a radial direction were picked up by a band receiver and displayed on cathode ray oscillographs and their amplitude distribution over the periphery was recorded with an x, y recording apparatus. Since only oscillations of the exciter frequency were taken into account in amplitude determination, the noncircularities of the cylinder do not show in the record. The natural frequencies at maximum amplitudes could be well determined by a vacuum tube voltmeter which indicated the dependence of the amplitudes on the exciter frequency.

/15

6. Results and Discussion

In Figure 4 the experimentally measured natural frequencies for a cylinder stiffened uniformly by 4 open profiles ($j = 4\pi$) are compared with the theoretical values (conversion matrix method). In contrast to the blur-calculated orthotropic cylinder (Figure 2) as well as to the isotropic cylinder, with the effect of longitudinal stiffening there are no pure cosine forms with n vibrations in the peripheral direction; rather eigenforms appear over the periphery, that are composed of trigonometric and hyperbolic components. Nevertheless basic cosine-like forms can be recognized (cf. also Figure 5) the number of whose vibrations over the periphery is designated " n ". The value " n " is plotted on the abscissa, and the natural frequencies f in Hertzian units are plotted on the ordinates. The indicated parameter is the number of half periods m in a

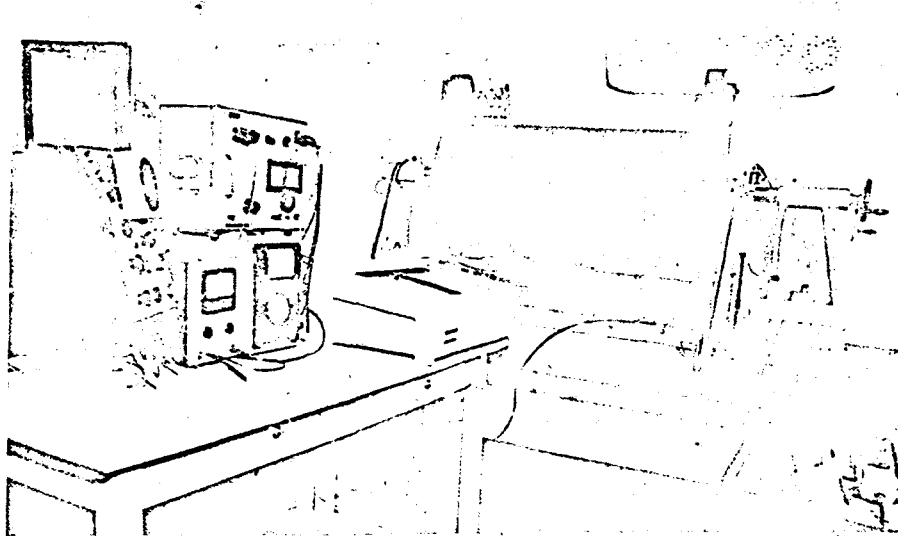


Figure 3. Experimental Apparatus

longitudinal direction. Dashed lines are supplied through the theoretical and experimental frequencies belonging to a specific m only for purposes of better orientation; such lines between integral " n " values physically have no meaning. /16

The characteristic of the "curves" is similar to that of the orthotropically calculated cylinder (Figure 2): for a specific m the frequencies decrease at first as " n " increases, later to increase again. With an increasing number of peripheral vibrations the elastic energy decreases and the bending energy increases. On the ascending branch of the "curve" the elastic energy prevails, and in the descending branch the bending energy prevails (cf. Ref. 1, p. 249), and thus the frequency characteristic is clarified. The least natural frequency at $m = 1$, " n " = 5 is approximately 90 Hz, and with an increasing number of longitudinal half periods the minima are displaced to greater " n ". The correlation between theory and experiment is very good, with the maximum deviation at $m = 4$, " n " = 10, circa 6 percent. For each curve there is displayed a theoretical value ($m = 1$, " n " = 10; $m = 2$, " n " = 4; $m = 3$, " n " = 6; $m = 4$, " n " = 9): the forms are illustrated in Figure 5. /17

Here theoretical eigenforms of a cylinder field ($j = 4\sqrt{1}$, $\varphi = 0 \div \pi/2$) are presented. Experimental values taken from the x , y recorder are drawn in for comparison.

Since the amplitudes of the eigenforms are determinable only up to one power, the theoretical values are so coordinated to the theoretical curves that the square of the deviation therefrom is a minimum. The experimental values conform very well with the course of the theoretical forms. At the beginning and end of the cylinder field the stringers are drawn so that those with horizontal tangents with equal amplitudes vibrate in the same or opposite direction and those with different amplitudes at the beginning and end of the field have different inclinations. Moreover the mentioned superposition of several components is to be observed in the forms.

In Table 1 the theoretical and experimental natural frequencies with the same number of stringers ($j = 4$) with different rigidities, four open ($\sqrt{1}$) and four closed (\square) profiles, are combined. The lines are differentiated according to the number of longitudinal half periods $m = 1 + 4$, and the columns according to the number of peripheral vibrations " n " = $4 + 12$. The theoretical values are shown in parentheses for purposes of comparison with experimental results. The correlation is good: the experimental values are somewhat below the theoretical frequencies throughout. In the case of a longitudinal half period ($m = 1$) the frequencies of the more rigid shell (4 closed profiles) lie below those of the less rigid cylinder (4 open profiles), the phenomenon being explained by the increased influence of the mass of the stringers. With larger m , effect of the increase of the stiffness prevails over that of mass, and the frequencies of the more rigid cylinder are higher.

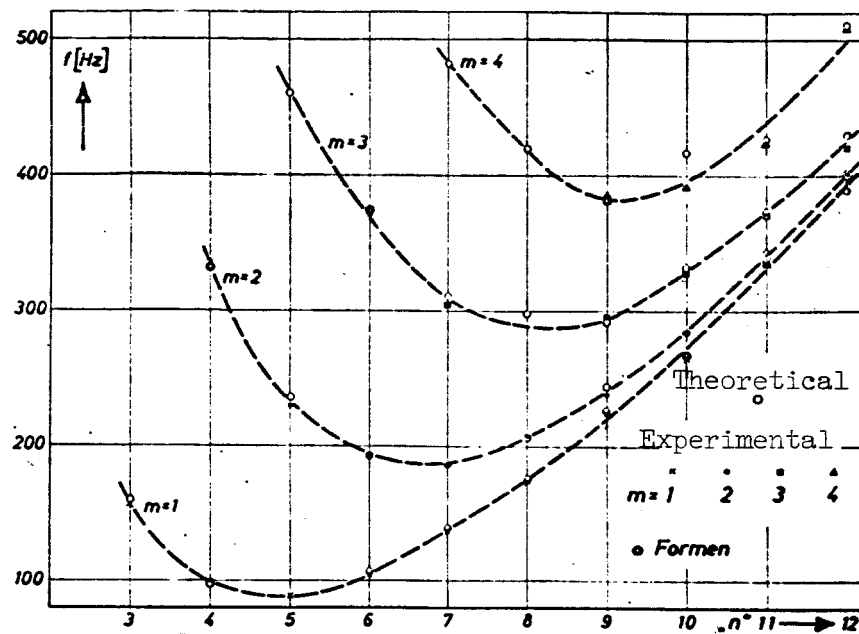


Figure 4. Theoretical and experimental natural frequencies of a stiffened cylinder ($j = 4$)

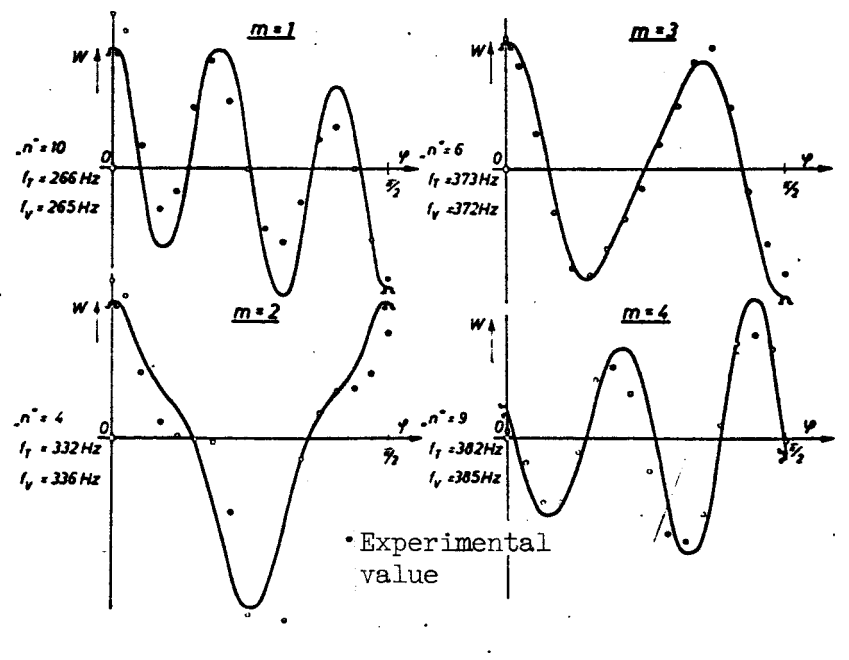


Figure 5. Eigenforms of a cylinder field with differing number of longitudinal half periods

Table 1. Natural Frequencies with Different Stiffenings
 $j = 4\pi, 4\pi$, Theory (Experiment)

/18

| $m \backslash n$ | 4 | 5 | 6 | 7 | 8 | 9 | 10 | 11 | 12 |
|------------------|-----------------|-----------|-----------|-----------|-----------|-----------|-----------|-----------|-----------|
| 1 | π 98 (100) | — (89) | 106 (104) | 139 (137) | 175 (174) | 226 (224) | 266 (265) | 336 (336) | 389 (396) |
| | π 101 (97) | — (90) | 107 (102) | 138 (134) | 171 (172) | 223 (218) | 253 (250) | 331 (325) | 377 (388) |
| 2 | π 332 (336) | 236 (229) | 193 (194) | 187 (187) | 206 (207) | 244 (238) | 285 (285) | 344 (336) | 401 (401) |
| | π 349 (328) | 242 (244) | 223 (206) | 199 (202) | 236 (220) | 270 (256) | 310 (288) | 352 (352) | 405 — |
| 3 | π | 460 — | 373 (372) | 311 (305) | 298 — | 292 (296) | 332 (329) | 374 (372) | 429 (421) |
| | π | 490 (482) | 462 (390) | 334 — | 336 (328) | 293 (314) | 340 (336) | 411 (418) | 504 (455) |
| 4 | π | | | 482 — | 420 — | 382 (385) | 417 (392) | 426 (425) | 511 (509) |
| | π | | | 492 — | 425 — | 385 (415) | 442 — | 434 (445) | — (455) |

Table 2. Natural Frequencies with Differing Numbers of Stringers $j = 0, 4\pi, 8\pi$, Theory (Experiment)

/19

| $j \backslash m$ | 4 | 5 | 6 | 7 | 8 | 9 | 10 | 11 | 12 |
|------------------|-----------|-----------|-----------|-----------|-----------|-----------|-----------|-----------|-----------|
| 0 | 100 (104) | 91 (92) | 110 (108) | 142 (140) | 183 (181) | 230 (229) | 284 (282) | 343 (340) | 409 (405) |
| 4 | 98 (100) | — (89) | 106 (104) | 139 (137) | 175 (174) | 226 (224) | 266 (265) | 336 (336) | 389 (396) |
| 8 | 94 (97) | — (86) | 105 (103) | 135 (133) | 164 (166) | 220 (217) | 266 (259) | 326 (325) | 371 — |
| 0 | 336 (358) | 234 (253) | 190 (200) | 185 (188) | 206 (208) | 244 (242) | 293 (291) | 350 (346) | 414 (404) |
| 4 | 332 (336) | 236 (229) | 193 (194) | 187 (187) | 206 (207) | 244 (238) | 285 (285) | 344 (336) | 401 (401) |
| 8 | 314 — | 234 (238) | 193 (192) | 188 (182) | 205 (198) | 240 (233) | 285 (281) | 336 (333) | 394 — |
| 0 | | 473 (505) | 356 (380) | 295 (309) | 275 (282) | 287 (297) | 320 (322) | 368 (369) | 427 (422) |
| 4 | | 460 — | 373 (372) | 311 (305) | 298 — | 292 (296) | 332 (329) | 374 (372) | 429 (421) |
| 8 | | — — | 373 (367) | 329 (311) | 317 — | 293 (297) | 332 (321) | 381 (370) | 430 (425) |
| 0 | | | | 459 (495) | 394 (415) | 369 (380) | 375 (387) | 406 (415) | 454 (458) |
| 4 | | | | 482 — | 420 — | 382 (385) | 417 (392) | 426 (425) | 511 (509) |
| 8 | | | | — (495) | 480 — | 402 (398) | 417 (415) | 439 (435) | 528 — |

If in the two observed cases of longitudinal stiffening the difference is not so great, particularly for frequency minima, the stiffening conformation as well as the limited number of stringers could be responsible.

Table 2 compares theoretical and experimental natural frequencies with differing numbers of stringers ($j = 4, 8$) of uniform conformation (open \sqcap profile) with the values of the isotropic cylinder ($j = 0$). The lines are again differentiated according to the number of longitudinal half periods $m = 1 + 4$ with subdivision according to the number of stringers $j = 0, 4, 8$: the columns indicate the number "n" of peripheral vibrations "n" = $4 + 12$.

For $m = 1$ the frequency diminishes at first with an increase in the number of stringers, a phenomenon that again is to be attributed to the greater influence of the increasing mass of the stringers. The same behavior is still to be observed at $m = 2$ with greater number of peripheral vibrations "n", while in the region of the minimum of the curve (frequency above "n") already a slight increase of frequency occurs with increasing number of stringers. This frequency increase is more pronounced with larger numbers of longitudinal half periods ($m = 3, 4$) because the bending stiffness of the stringers comes increasingly into play.

In addition to the given frequencies for the stiffened cylinder at which the stringers vibrate in resonance, the frequencies of the isotropic cylinder with even number "n" = 4, 6, 8, 10, 12 for $j = 4$ and "n" = 4, 8, 12 for $j = 8$ are also solutions of the problem of natural frequencies for stiffened cylindrical shells. With these "n" number of peripheral vibrations, the vibrational forms in the peripheral direction are so adapted that the stringers remain at rest.

/20

These frequencies for stringers at rest with even "n" were determined experimentally as well as with discrete calculation. They agree very well with the values of the isotropic cylinder obtained by calculation (blurred orthotropy at $j = 0$) and by experiment, but they are not presented here.

A comparison of the frequencies of the isotropic cylinder with those of the stiffened cylinder shows that with the present measurements the differences, especially for $m = 1$, and $m = 2$ are not very great.

In Figure 6 the natural frequencies of continuous calculation ("blurred orthotropy") are contrasted with the frequencies of discontinuous calculation (conversion matrices) for a cylinder stiffened by 8 open profiles ($j = 8n$). The former are interconnected by dashed lines for the number of longitudinal half periods m . For these frequencies the number of pure peripheral vibrations n are given as abscissa: n becomes "n" for discontinuous calculation as previously explained. In

addition as further solution the frequencies for the case of stringer at rest at "n" = 4, 8, 12 is drawn in, as well as all determined experimental values. /21

It is to be observed that for one and two half periods in the longitudinal direction the strict consideration of discrete stiffening has little advantage over blurred calculation. The frequencies according to the conversion matrix method only fall below those of blurred calculation as m increases: at m = 4 already around 10 percent. The few stringers applied to the skin in the approximation increase the theoretical stiffness of the vibrating cylinder to an unpermissible value. This effect that falsifies the results is naturally greater depending upon an increasing number of longitudinal half periods because thereby the bending stiffness of the stringer increases in its effect, whereby the frequencies are increased. Discrete calculation and experiment agree well also at high m. At m = 1 and m = 2 the results of blurred calculations do not deviate significantly from those of discontinuous calculation and are in the vicinity of the frequencies of the unstiffened shell. This indicates that here the effects of stiffness and vibrating mass of the stringer are almost nullified.

Precise investigation of the range of validity of calculation with blurred orthotropy must still be undertaken.

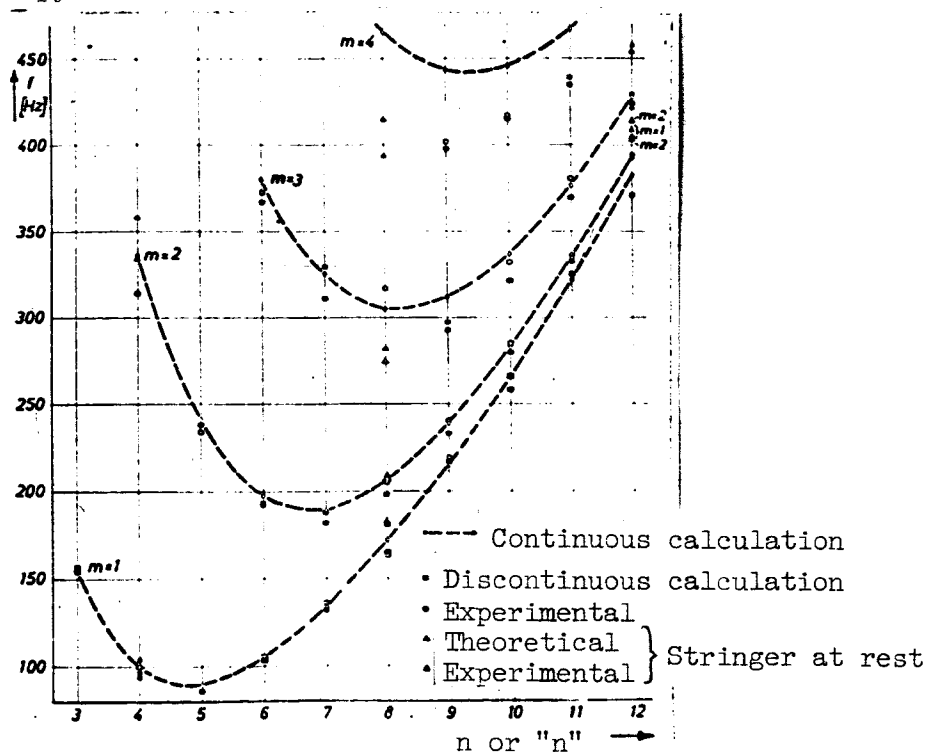


Figure 6. Natural frequencies in blurred orthotropy and matrix method ($j = 8\pi$)

The authors express their thanks to Mr. J. Martin, graduate engineer, for development of the measuring procedure, and Mr. H. Voigt, engineer, for carefully carrying out the experiment.

References

1. Arnold, R. N. and Warburton, G. B. Flexural vibrations of the walls of thin cylindrical shells having freely supported ends. Proc. Roy. Soc., London (A), Vol. 197, pp. 238-256, 1949.
2. Arnold, R. W. and Warburton, G. B. The flexural vibrations of thin cylinders. Inst. Mech. Eng. Proc. (A), Vol. 167, pp. 62-74, 1953.
3. Yu, Yi-Yuan Free vibrations of thin cylindrical shells having finite lengths with freely supported and clamped edges. J. Appl. Mech., Vol. 22, pp. 547-552, 1955.
4. Kozarov, M. Investigations of the oscillations of orthotropic shells (engl. Titel). Godishnik. Inzh.-stroit. in-t. Fak. stroit., arkhitekt., khidrotekhn., Vol. 10, (1), pp. 69-93, 1958.
5. Miller, P. R. Free vibrations of a stiffened cylindrical shell. A. R.C. A.1 Report 19, 338, L.A. 22, 1957.
6. Hoppmann, II, W. H. Flexural vibrations of orthogonally stiffened cylindrical shells. The Johns Hopkins University, Baltimore, Maryland.
7. Donnell, L. H. A new theory for the buckling of thin cylinders under axial compression and bending. Trans. Amer. Soc. Mech. Eng., Vol. 56, pp. 795-806, 1934.
8. Thielemann, W., Schnell, W. and Fischer, G. Beul- und Nachbeulverhalten orthotroper Kreiszylinderschalen unter Axial- und Innendruck (Bulging Behavior, and Post-Bulging Behavior of Orthotropic Circular Cylindrical Shells Under Axial and Internal Pressure). Z. Flugwiss. 8, pp. 284-293, 1960.
9. Flügge, W. Statik und Dynamik der Schalen (Statics and Dynamics of Shells). 3rd ed. Springer, Berlin, Göttingen, Heidelberg, p. 273 ff., 1962.

Translated for the National Aeronautics and Space Administration
by John F. Holman and Co. Inc.